An *in vitro* digestion study of encapsulated lactoferrin in rapeseed phospholipid–based liposomes

Daniela Vergara[a,b*], Olga López[d], Mariela Bustamante[b], Carolina Shene[b,c]

[a] *Doctoral Program in Sciences of Natural Resources, Universidad de La Frontera, Ave. Francisco Salazar 01145, Box 54-D, Temuco, Chile.*

[b] *Center of Food Biotechnology and Bioseparations, Scientific and Technological Bioresource Nucleus (BIOREN), Centre for Biotechnology and Bioengineering (CeBiB). Universidad de La Frontera, Ave. Francisco Salazar 01145, Box 54-D, Temuco, Chile.*

[c] *Department of Chemical Engineering, Universidad de La Frontera, Ave. Francisco Salazar 01145, Box 54-D, Temuco, Chile.*

[d] *Department of Chemical and Surfactant Technology, Institute of Advanced Chemistry of Catalonia (IQAC-CSIC), C/Jordi Girona 18-26, 08034, Barcelona, Spain.*

This manuscript has not been submitted for publication in another journal.

*Corresponding author: Tel.: +56 45 2325491; fax: +56 45 2732402

E-mail address: d.vergara02@ufromail.cl (D. Vergara).

Highlights

- Rapeseed phospholipids (RP) liposomes were used to encapsulate lactoferrin (LF).
- Liposomal integrity was more affected by gastric than by intestinal digestion.
- Liposomes delayed the LF hydrolysis under gastric and intestinal digestion.
- LF accelerates the release of FFAs depending on liposome formulation.
- Liposomes formulation for oral delivery system of LF are suggested.

Abstract

Effectiveness of liposomes elaborated with rapeseed phospholipid (RP) extracted from a residue of oil processing, stigmasterol (ST) and/or hydrogenated phosphatidylcholine (HPC) for the encapsulation lactoferrin (LF) was studied; lipid membrane of liposomes was characterized (bilayer size, chain conformational order, lateral packing, lipid phase, and morphology) and the protection offered to the encapsulated LF during *in vitro* digestion was determined. Liposomes composed of RP+ST$^{LC\ (low\ concentration)}$ showed spherical and irregular vesicles without perforations. Lamellar structure was organized in a liquid–ordered phase with a potential orthorhombic packing. Stability and size of the liposomes were more affected by gastric digestion than intestinal digestion; 67–80% of the initially encapsulated LF remained intact after gastric digestion whereas the percentage was reduced to 16–35% after intestinal digestion. Our results shows that liposomes elaborated with RP, properly combined with other lipids, can be a useful oral delivery system of molecules sensitive to digestive enzymes.

Keywords: Rapeseed phospholipids, liposomes, lactoferrin, digestion, delivery system.

Abbreviations: LF, lactoferrin; **RP,** rapeseed phospholipids; **ST,** stigmasterol; **HPC,** hydrogenated phosphatidylcholine; ^{LC}**,** low concentration; **SAXS,** small angle X–ray scattering; **WAXS,** wide angle X–ray scattering; **DSC,** differential scanning calorimetry; $\mathbf{T_m}$**,** gel to liquid main transition temperature; **cryo–TEM,** cryogenic transmission electron microscopy; **EE,** encapsulation efficiency; **GF,** gastric fluid; **IF,** intestinal fluid; **DG,** gastric digestion; **ID,** intestinal digestion; **PDI,** polydispersity index; **SDS–PAGE,** sodium dodecyl sulfate polyacrylamide gel electrophoresis; **FFA,** free fatty acid.

Introduction

Lactoferrin (LF) is a natural iron–binding glycoprotein (molecular weight ~78-80 kDa, ~700 amino acids), mainly present in milk and also secreted through fluids of mammals. LF not only participates in the transport of iron but is also a prebiotic protein with a wide range of physiological functions; it is considered an important defense molecule because of its antibacterial and antifungal activity (Iglesias-Figueroa, Espinoza-Sánchez, Siqueiros-Cendón, & Rascón-Cruz, 2019). However, oral delivery of LF decreases most of its functions due to enzymatic degradation in the gastrointestinal tract, resulting in less than 1% absolute oral LF bioavailability levels (Troost, Saris, & Brummer, 2002), hindering its potential benefits. LF degradation has led the research of new forms of protection, with the aim of decreasing its hydrolysis after oral administration (Yao, Bunt, Cornish, Quek, & Wen, 2015).

Encapsulation is a powerful tool for overcoming the aforementioned drawbacks. Encapsulation offers immobilization, protection against environmental factors (light, temperature, pH, moisture, and oxygen), controlled release, structure, and functionalization for sensitive compounds, increasing their bioavailability (Jafari & McClements, 2017). Recent studies in the food and nutrition have considered the utilization of liposomes to encapsulate and control the release of bioactive components, such as antioxidants, fatty acids, and proteins (Gibis, Ruedt, & Weiss, 2016; Vélez, Perotti, Zanel, Hynes, & Gennaro, 2017; Liu, Ye, Liu, Liu, & Singh, 2013). Liposomes are small and spherical vesicles (20 nm to 2 µm in size), formed by hydrophilic–hydrophobic interactions that occur between phospholipids, cholesterol, and water molecules (Zhang, Pu, Tang, Wang, & Sun, 2019a). Cholesterol is an important component of liposome membranes; in cell membranes

89 cholesterol reduces the rotational freedom of the phospholipid hydrocarbon chains,
90 stabilizes the lipid bilayer, and helps to decrease the loss of hydrophilic materials
91 (Kaddaha, Khreich, Kaddah, Charcosset, & Greige-Gerges, 2018) especially in fluid lipid
92 membranes. Jovanović et al. (2018) established that plant cholesterol or phytosterols (β–
93 sitosterol, stigmasterol, and campesterol) not only act as stabilizers in liposomal
94 membranes, but also as antioxidants, enhancing the protection role of liposomes

95 Liposomes can be manufactured using phospholipids extracted from plant raw materials,
96 which allows an easy and fast implementation in food systems, surpassing the established
97 regulatory barriers (Sun, Chen, Wang, & Lin, 2018). Phospholipids from plant sources, for
98 example of rapeseed, can be found as a by–product of the oil refining process. Recently, we
99 showed that RP can be used for developing LF–loaded liposomes with a high encapsulation
100 efficiency (EE, ~90 %) in small particles (<200 nm) (Vergara & Shene, 2019).

101 For the successful use of LF–loaded into RP based liposomes as a food ingredient, not
102 only optimal processing conditions need to be determined but evidence of the protection
103 offered to LF after its consumption has to be demonstrated. It has been shown that LF–
104 loaded liposomes prepared with milk derived phospholipids, may prevent gastric
105 degradation of LF and reduce the rate of hydrolysis of LF under intestinal conditions (Liu
106 et al., 2013). Niu et al. (2019) reported that encapsulation of LF does not compromise its
107 antimicrobial bioactivity. To our knowledge, the fate of LF encapsulated in RP–liposomes
108 during *in vitro* gastrointestinal digestion, which is important for the effective use of
109 liposomes, has not been determined.

110 Recently, we have carried out a detailed characterization of RP and RP–liposomes
111 (chemical composition, physical stability, appearance, and storage effects among other); in

addition, conditions that maximize LF encapsulation efficiency (EE) were determined (Vergara & Shene, 2019). Thus, to extend our previous work the aims of the present study were (1) to characterize the lipid membrane of RP–liposomes, (2) to evaluate the protection offered to LF encapsulate in different formulations of RP–liposomes during *in vitro* digestion, and (3) to determinate the lipid composition of RP–liposomes to achieve the best protection of LF during *in vitro* digestion. These results could contribute for the development of an effective system for the oral delivery of LF that could be used in nutraceutical and functional products.

2. Materials and methods

2.1. Materials

Rapeseed oil was obtained from the residue left after cold pressing process carried out by OleoTop S.A. (Freire, Araucania Region, Chile). Composition of the oil residue can be found in the supplemental data file (Supplementary Data 1.docx). Rapeseed phospholipids (RP) were extracted following the methodology described in our previous study (Vergara & Shene 2019). Stigmasterol was purchased from Sigma–Aldrich (St. Louis, MO, USA). Hydrogenated soy phosphatidylcholine (HPC) (Phospholipon® 90H) was supplied from Lipoid GmbH (Ludwigshafen, Germany). Lactoferrin was purchased from Jarrow Formulas, (Los Angeles, California, USA). Pepsin from porcine gastric mucosa (enzymatic activity of 3,200–4,500 U/mg protein) pancreatin from porcine pancreas (4 × United States Pharmacopeial (USP) specifications) and bile bovine were purchased from Sigma–Aldrich (St. Louis, MO, USA). All chemicals and solvents used were of analytical or HPLC grade.

135 *2.2. Preparation of liposomes*

136 Liposomes with the different compositions defined in Table 1 were prepared by the
137 thin–layer dispersion method. The optimal formulation, based on the desirable quality
138 attributes (high EE and small particle size) described previously (Vergara & Shene, 2019)
139 was used as a starting point. Briefly, RP (10.20 mg/mL) and stigmasterol (ST; 2.20 mg/L,
140 cholesterol of plant origin) dissolved in chloroform (2 mL) were placed into a round–
141 bottom flask. The solvent was removed in a rotary evaporator (Buchi R–100, Flawil,
142 Switzerland) at 40 °C; a thin lipid film was formed on the flask walls. To ensure the
143 complete removal of the dissolvent from the film, the round–bottom flask was left
144 overnight inside a vacuum desiccator. Then, the dried lipid film was rehydrated with
145 phosphate buffer (pH 7.4, 0.01 M), containing LF at 1 mg/mL and subjected to sonication
146 using a bath sonicator Ultrasons H–D (P–Selecta, Barcelona, Spain) during 4 min. For
147 liposomal membrane characterization liposomes were prepared without LF. Finally,
148 liposomal formulations were maintained 24 h at room temperature to ensure hydration. This
149 formulation was named RP+ST$^{low\ concentration\ (LC)}$.

150

151 *2.3. Characterization of the structure of RP+ST^{LC} liposomes*

152 To evaluate the physicochemical characteristics of the RP+ST^{LC} liposomes and the effect
153 of enzymatic digestion on the vesicular structure, several techniques were used.

154

155 *2.3.1. Small angle X–ray scattering (SAXS)*

SAXS measurements of the RP+ST^{LC} liposomes were carried out using a S3–MICRO (Hecus X–ray systems GMBH Graz, Austria) coupled to a GeniX Cu high flux source (Xenocs, Grenoble). X–ray radiation with a wavelength corresponding to a Cu–Kα source (1.542 Å) was used. Transmitted scattering was detected using a PSD 50 (Hecus; Graz, Austria), and the temperature was controlled by means of a Peltier TCCS–3 (Hecus GmbH; Graz, Austria). The sample was inserted in a flow–through glass capillary (Hilgenberg GmbH; Malsfeld, Germany) with a 1 mm diameter and 10 mm wall thickness. The scattering intensity I (in arbitrary units) was measured as a function of the scattering vector Q (in reciprocal Å) defined through:

$$Q = (4\pi \sin\theta)/\lambda \quad \text{(Eq. 1)}$$

Where θ is the scattering angle and λ is the wavelength of the radiation (1.542 Å). The position of the scattering peaks is directly related to repeat distance of the molecular structure, as described by Bragg's law (Bragg, 1913):

$$2d \sin\theta = n\lambda \quad \text{(Eq. 2)}$$

Where *n* and *d* represent the order of the diffraction peak and repeat distance, respectively. In a lamellar structure, the various peaks are located at equidistant positions; the position of the nth order reflection, Qn is given by:

$$Qn = 2\pi n/d \quad \text{(Eq. 3)}$$

2.3.2. Differential scanning calorimetry (DSC)

DSC measurements were performed using a calorimeter (Mettler Toledo 821E, Greifensee, Switzerland). Samples were concentrated by centrifugation at 9,000 × g for 10 min to increase the signal intensity. Aliquots of ~10 μL were placed inside aluminum DSC pans and sealed hermetically. The scan rates for heating and cooling were 5 °C/min and −5 °C/min, respectively, over a temperature range from –60 to +60 °C. The DSC curves were analyzed by the STARe SW 9.30 Software (Mettler Toledo, Greifensee, Switzerland). The curve shown in result section correspond to the second heating scan.

2.3.3. Cryogenic transmission electron microscopy (cryo–TEM)

The morphology of the RP+ST^{LC} liposomes was evaluated by cryo–TEM. Samples (~3 μL) were applied on a holey carbon grid. The blotted grids were plunged into liquid ethane cooled with liquid nitrogen using a Vitrobot (FEI Company, Eindhoven, The Netherlands). The vitreous sample film was transferred to a Tecnai F20 TEM (FEI Company, Eindhoven, The Netherlands) microscope using a cryotransfer holder (Gatan, Pleasanton, USA). Images were acquired at 200 kV at a temperature between 170 ºC and 175 ºC, under low–dose imaging conditions. Images were recorded with a CCD Eagle camera (FEI, Eindhoven, The Netherlands) and processed with Xplore3D software (FEI Eindhoven, The Netherlands).

2.4. In vitro digestion of liposomes

2.4.1. Stability of liposomes under gastric and intestinal digestion

197 The simulated gastric fluid was prepared by dissolving NaCl (2 g) and HCl (7 mL) in 1
198 L of deionized water. Composition of the simulated intestinal fluid was K_2HPO_4 6.8 g/L,
199 NaOH 190 mL of 0.2 M solution/L, NaCl 150 mM, $CaCl_2$ 30 mM, and bile extract 0.1 g/L
200 in deionized water.

201 RP+ST^{LC} liposomes were incubated separately in gastric fluid, intestinal fluid, gastric
202 fluid + pepsin (defined as, *gastric digestion*), and intestinal fluid + pancreatin (defined as,
203 *intestinal digestion*), according to the methodology described by Liu et al. (2013). Pepsin
204 57 ng/mL, and pancreatin 0.015 mg/mL at a 2:1 v/v ratio (3 mL total) were used. The pH of
205 the samples in the simulated gastric and intestinal fluids were adjusted to 1.5 and 7.4
206 respectively; 0.05 M NaOH or 1 M HCl were used as needed. The mixtures were incubated
207 with agitation (Unitronic 320 P–Selecta, Barcelona, Spain) (30 rpm; at 37 °C); 200 µL of
208 the sample were taken for analysis after 1, 30, and 120 min. Particle size, polydispersity
209 index (PDI), and ζ–potential of RP+ST^{LC} liposomes in the gastric and intestinal fluid, and
210 during gastric and intestinal digestion were followed in time, using a Zetasizer Nano ZS
211 (series HT, Malvern Instrument, U.K.) at 25 °C; measurement conditions were defined
212 according to Zhang et al. (2019b).

213

214 *2.4.2. Enzymatic digestion of LF–loaded into different liposome formulations*

215 The different formulations subjected to *in vitro* gastrointestinal digestion (Table 1)
216 were: (1) RP+ST^{LC}; (2) liposomes in which RP and ST concentrations were 2.5–fold higher
217 (named as RP+ST), (3) liposomes in which ST was replaced by hydrogenated
218 phosphatidylcholine (HPC) (named as RP+HPC), and (4) liposomes in which the mass ratio

of RP: HPC: ST was 70:20:10 (named as RP+HPC+ST). The digestion of free LF and LF–loaded into RP+ST^{LC}, RP+ST, RP+HPC, and RP+HPC+ST liposomes was carried as described in section 2.4.1. Digested samples were placed in vials, where the enzymes were inactivated with SDS–PAGE loading buffer (62.5 mM Tris–HCl pH 6.8, 20% glycerol, 2% SDS, 0.1% bromophenol blue and 5% β–mercaptoethanol) added in a volume ratio of 2:1 v/v. The mixtures were stored at –20 ºC until loading onto the SDS–PAGE gel.

2.4.3. Protein hydrolysis kinetics by SDS–PAGE

To determine the hydrolysis degree of the encapsulated LF incubated with the gastric and intestinal fluid, and after gastric and intestinal digestion, the quantity of not hydrolyzed LF was determined by SDS–PAGE using a 15% w/w polyacrylamide gel as described by Laemmli (1970). The gels were run in a Mini–Protean Tetra System (BioRad, USA) at 130 V using a Bio–Rad power supply unit PowerPac^{TM} (BioRad, USA). Gels were stained (1.25 g/L Coomassie Blue R–250 in ethanol: glacial acetic acid: water at 52: 10: 38 v/v/v) for 120 min and then distained (ethanol: glacial acetic acid: water at 26: 0.8: 73.2 v/v/v). PageRuler™ Unstained Protein Ladder (Thermo Scientific; 10 to 250 kDa) was used as molecular weight marker. Gel images were acquired using a RICOH MP–C3003 Photo Scanner. The relative percentages of LF in the samples (compared with the LF standard) was quantified using ImageJ 1.50i (NIH, USA) software.

2.4.4. Lipolysis of LF–loaded liposomes

In vitro lipid digestion was monitored as described by De Figueiredo, Guedes, Paim, and Lopes (2018). RP+ST^{LC}, RP+ST, RP+HPC, and RP+HPC+ST liposomes all of them loaded with LF, and liposomes without LF (2 mL) were mixed with 5 mL of intestinal fluid and the pH was adjusted to 7.4. Lipolysis of phospholipids was determined by the pH–stat titration technique after the addition of pancreatin (0.015 mg/mL). Briefly, the pH was maintained at 7.4 (Orion Star^{TM} A211, Thermo-Scientific) through the addition of 0.05 M NaOH, under continuous magnetic stirring (100 rpm at 37 ºC). The volume of NaOH added was used to calculate the concentration of free fatty acids (FFAs) released using:

$$\boldsymbol{FFA}\ (\boldsymbol{mM}) = (V_{NaOH\ t} - V_{NaOH\ to})\ x\ M_{NaOH}\ x\ 1000 \qquad \text{(Eq. 4)}$$

Where: $V_{NaOH\ t}$ is the volume (L) of NaOH required to titrate the FFAs produced after 30 min, $V_{NaOH\ t0}$ is the volume (L) of NaOH added at the beginning of the reaction, and M_{NaOH} is the molarity (M) of the NaOH solution.

2.5. Data analysis

All measurements were repeated at least three times. The results were evaluated statistically for significance ($P<0.05$) using ANOVA and the Tukey means comparison test Minitab® software version 18 (State College, PA, USA) was used. All data were expressed as means ± standard deviations.

3. Results and discussion

3.1. Characterization of the RP+ST^{LC} liposomes

3.1.1. X–ray scattering

SAXS method was applied to gain insight into the structural organization of RP+ST^{LC} liposomes. SAXS provides information on the larger structural units of a given sample. In our case, the lamellar repeat distance (*d–spacing*) was estimated from analysis of the peaks using Bragg's law and was attributed to the thickness of the liposomes bilayer. Results are shown in Fig. 1a. One broad reflection was observed, at a *q* around 0.10 Å^{-1}, corresponding to a *d* value around 63 nm, which was attributed to the thickness of the lipid bilayer. In addition, SAXS may also be used to provide an indication of the lamellarity of a liposome population (Kiselev & Lombardo, 2017). Shape of the SAXS patterns, was very broad and with only one symmetric peak which does not show other reflections, this can be associated with unilamellar liposomes (Rodríguez et al., 2012). In general, SAXS from multilamellar liposomes exhibit first and second order diffraction peaks at regular intervals that is 1/*d*; 2/*d*, etc. (Andrade et al., 2018).

Wide angle X–ray scattering (WAXS) provides information about the scattered intensity at angles wider than SAXS. Thus, information on smaller structural units in the sample, such as lateral packing in the lamellar phase can be acquired. Fig. 1b shows WAXS profile for RP+ST^{LC} liposomes. Two possible reflections were observed at 1.50 Å^{-1} and 1.70 Å^{-1}. This reflection could correspond to Bragg distances at approximately 4.2 and 3.7 nm, respectively. It is known that lipids are able to exhibit different lateral symmetry that give rise to determine *d*–spacing in WAXS profile. This lateral packing can be orthorhombic (*d*–spacing at 41 and 37 nm), hexagonal (41 nm), or liquid–disordered (46 nm) (Rodríguez et al., 2012). WAXS pattern on Fig. 1b shows *d*–spacing that could be ascribed to an orthorhombic organization. In our case, the complex composition of the phospholipids (RP) (Vergara & Shene, 2019) used for liposomes preparation, related to extension of the alkyl

chain and presence of unsaturations, could alter both the tendency for monolayer curvature, and the packing stresses within the system (Gupta, De Mel, & Schneider, 2019).

3.1.2. Differential scanning calorimetry (DSC)

DSC analysis was performed to determine the liquid–crystalline phase transition temperature (T_m) of the lipid phase in RP+ST^{LC} liposomes. Phospholipids forming bilayers have a specific T_m depending on the length and saturation degree of the alkyl chain. When temperature exceeds T_m, the gel to liquid–crystalline phase transition occurs, and lipid membranes experience some physicochemical changes (Romero-Arrieta, Uria-Canseco, & Perez-Casas, 2019). In the calorimetric study, both cooling and heating curves were determined for the RP+ST^{LC} liposomes (Fig. 1c). No peaks associated with a main lipid transition were observed in the temperature range studied (–60 to +60 °C); the peak at approximately 5 °C corresponded to ice melting. Thus, we assumed that the main transition was suppressed in the system studied. This suppression could be related with the inclusion of stigmasterol (and other sterols) in phospholipid membranes. Rodríguez et al. (2012) working with membranes elaborated with 2–dimyristoyl–sn–glycero–3–phosphocholine (DMPC) and cholesterol sulphate (SCHOL) reported the formation of an extra lamellar phase, "the liquid–ordered phase", with characteristics between solid ordered (gel) and liquid disordered phases. A similar phenomenon was described by Neunert et al. (2018) that incorporated α–tocopherol in 1,2-dipalmitoyl-sn-glycero-3-phosphocholine (DPPC) liposomes. To evaluate the possible effect of ST, and for comparison purposes, DSC analysis of RP liposomes without the inclusion of ST was determined. Heating thermogram, shown in Fig. 1d did not show peaks related with T_m it could not be discarded

the effect of endogenous α– γ– and δ–tocopherols content of RP (77.67 mg/100 g) (Vergara & Shene, 2019), on the order–disorder of the bilayer and decreasing the enthalpy of the main transition. Therefore the presence of this phase would not imply significant conformational changes; these results were as expected on the basis of the origin of the phospholipid fractions used.

3.1.3. Cryogenic transmission electron microscopy (cryo–TEM)

The microstructure of the RP+ST^{LC} liposomes was observed using cryo–TEM; images are shown in Fig. 1e–f. In general, images showed unilamellar vesicles, which is highly consistent with the SAXS results. The cryo–TEM analysis revealed nano–sized vesicles with diameters lower than 200 nm. In addition, vesicular shaped structures as well as, irregulars, cochleates, or elongated lipid assemblies were observed (Fig. 1e); these are usually made of negatively charged phospholipids and cations. The formation of these structures would be due to the different distribution of the RP in the different aggregates (Rahnfeld, Thamm, Steiniger, van Hoogevest, & Luciani, 2018). Fig. 1f shows liposomes in close contact (see arrow) that are deformed at the contact area. This could indicate a "flaccid" membrane character with domains of low rigidity given by lipid irregular distribution in the liposomal structure. In addition, according to the WAXS and DSC results that suggest an orthorhombic structure and a liquid–ordered phase respectively, the distribution of phospholipids and sterols in domains of different stiffness is also evidenced. One important result of the morphological analysis is the absence of irregularities such as perforations and/or breakages, in the bilayer membranes of the vesicles.

330

331 *3.2. Physicochemical stability of RP+ST^{LC} liposomes during in vitro digestion*

332 RP+ST^{LC} liposomes were incubated separately in gastric fluid, intestinal fluid, gastric
333 fluid + pepsin (*gastric digestion*), and intestinal fluid + pancreatin (*intestinal digestion*)
334 respectively. Physicochemical behavior (particle size, PDI, and ζ–potential) was followed
335 as a function of time (0–120 min). These experiments were carried out to check the
336 effectiveness and stability of the lipid membrane of liposomes not loaded with LF under
337 gastrointestinal conditions. Results showed that particle size of the liposomes increased
338 during *in vitro* digestion (Fig. 2a–f); average particle size of RP+ST^{LC} liposomes (291.47 ±
339 4.63 nm) increased 1.4–fold after the incubation with the gastric fluid, and 1.7–fold after
340 gastric digestion. For the intestinal conditions, the average particle size of RP+ST^{LC}
341 liposomes (initially equal to 312.03 ± 2.29 nm) increased 1.3–fold after the incubation with
342 the intestinal fluid, and 1.4–fold after intestinal digestion. The changes in particle size of
343 liposomes correlated with changes in PDI values. ζ–potential of RP+ST^{LC} liposomes
344 increased from –8.07 ± 2.02 mV to –1.96 ± 0.98 mV after the incubation in the gastric
345 fluid; and to –2.50 ± 0.56 after gastric digestion. Non–significant differences were observed
346 in the changes of ζ–potential of the RP+ST^{LC} liposomes exposed to intestinal conditions;
347 average initial value was –10.70 ± 1.21 mV that decreased to –11.19 ± 1.99 mV after the
348 incubation in the intestinal fluid and to –11.48 ± 0.18 mV after intestinal digestion.

349 The observed increase in the average particle size of RP+ST^{LC} liposomes during
350 digestive conditions suggests possible vesicle aggregation or fusion. This fact could be due
351 to the important decrease in pH from neutral (pH 7.4 liposomal formulation) to strongly
352 acid (pH 1.5) during gastric phase; changes in the pH modify the strength and range of

colloidal interaction between particles, allowing liposome coalescence. Additionally, an osmotic effect due to the pH gradient (inside - outside the vesicles) could promote destabilization and fusion. The increase in the average particle size of RP+ST^{LC} liposomes is in accordance with the results reported by Machado, Pinheiro, Vicente, Souza–Soares, and Cerqueira (2019) for liposomes elaborated with rice and soybean phospholipids for the encapsulation of phenolic extracts. However, Liu et al. (2013) reported that during *in vitro* gastrointestinal digestion of LF–loaded liposomes, prepared with milk fat globule membrane phospholipids, particle size decreased. So, the structure of different liposomal systems would present a different behavior due to the different conditions (pH and temperature) of digestion process. Studies carried out to solubilize liposomes with bile salts and other surfactants, reported an initial increase in size followed by a decrease (López et al., 1998). Then, foreseeable variations in size are certainly expected.

The electronegative ζ–potential value registered in the initial formulations is due to phosphate groups (PO_4^{3-}) in phospholipids (Liu et al., 2013). In addition, the presence of impurities in RP, such as FFA and amino acids, might also contribute to the electronegative ζ–potential of liposomal formulations (McClements, 2016). A high absolute value (higher +/– 30 mV) of ζ–potential indicates that liposomes are more electrically and physically stable. In our case, the low absolute values obtained suggest low stability of the liposomal formulation. In addition, the ζ–potential value under intestinal digestion could be attributed to the presence of the different anionic particles in the intestinal fluids (such as bile salts) or due to lipid digestion products, such as FFAs. Additionally, lysophospholipids in RP or those originated in phospholipid lipolysis, have a charge more negative than the parent lipids, which would also increase the negative charge of the liposomes (Zhang et al.,

2019a). Overall, physicochemical results indicated that the integrity and stability of RP+ST^{LC} liposomes was more affected by gastric digestion than by intestinal digestion, however in both digestions vesicular structures persisted.

3.3. Stability of encapsulated LF during in vitro digestion of LF–loaded in different liposomal formulations

The SDS–PAGE was used to evaluate the hydrolysis of LF, free and encapsulated into RP+ST^{LC}, RP+ST, RP+HPC, and RP+HPC+ST liposomes during *in vitro* gastrointestinal digestion. LF–loaded into RP+ST^{LC} liposomes was almost completely degraded under gastric digestion; only 20.48 ± 3.57% of the initial LF remained after 120 min of digestion (Table 2). Taking into account the "liquid–ordered phase" of the of RP+ST^{LC} liposomes membrane, a saturated phospholipid (HPC) was used in the liposome formulation to increase the rigidity and stability of the liposomal membrane.

Fig. 3a–b shows compares the intensity of the protein bands of LF standard and liposome samples after gastric and intestinal digestion (0–120 min) separated by SDS-PAGE. LF standard showed one strong band near 78–80 kDa, and some minor bands visible around 55, 35, and 15 kDa, which might be residual proteins remaining from the protein purification. The relative percentages of LF in the samples (compared with the standard LF) are summarized in Table 2. Free LF was totally hydrolyzed after 120 min of gastric digestion. LF in RP+ST^{LC}, RP+ST, RP+HPC, and RP+HPC+ST liposomes decreased gradually under gastric digestion as time increases (0 to 120 min) (Fig. 3a). After 120 min of gastric digestion the percentage of residual LF in RP+ST (67.49 ± 1.79%),

398 RP+HPC (79.98 ± 1.82%), and RP+HPC+ST (69.99 ± 0.99%) liposomes was significantly
399 ($P<0.05$) higher than in RP+ST^{LC} liposomes (20.48 ± 3.57%). During intestinal digestion of
400 free LF, hydrolysis occurred mainly during the first seconds (Table 2). Pancreatin and bile
401 salts were responsible of the significant solubilization of the liposomal membrane and
402 reduced amounts of LF remained in RP+ST^{LC} (10.88 ± 0.60%), RP+ST (34.80 ± 0.65%),
403 RP+HPC (32.19 ± 1.87%), and RP+HPC+ST (15.85 ± 1.56%) liposomes, after 120 min of
404 digestion. Nevertheless, LF encapsulated in RP+ST and RP+HPC liposomes resisted the
405 hydrolysis better than free LF (10.18 ± 1.10%).

406 The improved performance exhibited by the new liposomal formulations, especially
407 RP+HPC liposomes, under gastric digestion could be related to the encapsulation and the
408 load capacity of the vesicles. Under gastric conditions LF would be positively charged
409 whereas the liposomes would be negatively charged, suggesting that unloaded LF could
410 cover the liposomes surface by electrostatic interactions (Liu, Wei, Ye, Tian, & Han, 2017).
411 The comparison of results obtained with RP+ST^{LC} and RP+ST suggests that increasing the
412 concentration of phospholipids in liposomal formulations increases the percentage of LF
413 effectively encapsulated, delaying the protein hydrolysis by pepsin. During the intestinal
414 digestion, the presence of bile salts, phospholipids free or hydrolyzed, and fatty acids may
415 form mixed micelles or different complexes protecting LF from hydrolysis. The
416 composition of the liposomal wall is another factor that can significantly influence the
417 behavior of liposomes during digestion. Liu et al. (2017) determined that the addition of
418 cholesterol in phospholipid bilayers improves the stability of liposomal membranes under
419 *in vitro* gastrointestinal conditions. However, our results using ST (a plant cholesterol) are
420 not superior to those obtained incorporating HPC into the liposome formulation. Maherani,

421 Arab–Tehrany, Kheirolomoom, Geny, and Linder (2013) established that liposomes
422 prepared with lipids having low T_m values exhibited a greater permeability. Therefore,
423 lipids with higher T_m such as HPC (T_m ~55 °C) used in our formulations can form more
424 stable and less permeable liposomes, preventing the hydrolysis of LF. One characteristic of
425 RP is the high percentage of unsaturated fatty acids; percentages of oleic (C18:1), linoleic
426 (C18:2), and α–linolenic (C18:3) acid are 55.02 ± 0.06%, 27.97 ± 0.07%, and 6.26 ±
427 0.01%, respectively (Vergara & Shene, 2019). Maherani et al. (2013) reported that the
428 increase of unsaturation in the lipids of the liposomal bilayer increases the fluidity of the
429 liposomal membrane. However, unsaturated fatty acids would make artificial membrane
430 more permeable. This would explain the better results obtained with liposomes
431 formulations containing HPC (mixture that has 85% of 1,2–distearoyl–sn–glycero–3–
432 phosphocholine (18:0 DSPC) and 15% of 1–palmitoyl–2–stearoyl–3–phosphocholine (16:0
433 PSPC).

434 LF free and loaded into RP+ST^{LC}, RP+ST, RP+HPC, or RP+HPC+ST liposomes
435 incubated in gastric or intestinal fluid showed a lower initial percentage of LF compared
436 with LF standard (which corresponds to 100%). This loss could be due to two factors, (1)
437 the action of non–enzymatic components of the gastric or intestinal fluid (pH 1.5 and 7.4,
438 respectively) on the protein and/or (2) the conditions used in the elaboration of LF–loaded
439 liposomes such as, temperature and sonication. In the case of RP+ST^{LC} liposomes
440 incubated in the intestinal fluid, LF percentage was lower than in free LF. This could be
441 due to the molar relation between bile extract and phospholipids used. By increasing the
442 bile salt concentration, the vesicles become saturated with bile salt molecules and bile salt
443 partitioning to phospholipid membrane occurred. Kokkona, Kallinteri, Fatouros, and

444 Antimisiaris (2000) observed that at a higher molar ratio of bile extract: phospholipids
445 liposomes were more unstable releasing 100% of the encapsulated compound. In our study,
446 the non–encapsulated LF could surround the liposomal membrane affecting the digestion
447 rate of the liposomes by pancreatin through competitive absorption process (Meshulam &
448 Lesmes, 2014).

449 During the *in vivo* digestion, hydrolysis and absorption of nutrients in the small intestine
450 occurs simultaneously. Destabilization of the liposomal membrane is necessary for that the
451 released LF can reach the intestinal mucosa and be taken up by enterocytes. In addition, it
452 is well known that the mean residence time of a formulation administered orally is well
453 over 120 min in the small intestine (Boland, 2016). Therefore, it is important to obtain
454 percentages of intact LF higher than 30% after 120 min under intestinal digestion. The
455 non–gradual reduction of the percentage of LF remaining under intestinal digestion in
456 RP+ST and RP+HPC liposomes is attributable to the condition of the digestion assay. The
457 presence of diffuse bands as well as, the interference caused by the intestinal fluid, which
458 generates precipitates could affect the homogeneous sampling. After 120 min under
459 intestinal digestion, the system was found to be more homogenous due to the agitation and
460 temperature (100 rpm, 37 °C) therefore, the generated band is sharper.

461 Our results shows that RP+HPC liposomes can be very useful systems for the oral
462 delivery of LF, because nearly 80% of the LF remained intact after 120 min of gastric
463 digestion. This result is compared with the less than 1% absolute oral bioavailability of free
464 LF reported by Troost, Saris, & Brummer, (2002).

465

3.4. In vitro lipid digestion under intestinal digestion

Pancreatin lipolysis of phospholipids in RP+ST^{LC}, RP+ST, RP+HPC, and RP+HPC+ST liposomes under intestinal digestion was quantified indirectly measuring the concentration of released FFAs (Fig. 4). Loaded LF had a significant effect on the amount of FFAs released from RP+ST and RP+HPC+ST liposomes ($P<0.05$). On the contrary, the effect of loaded LF on the FFAs released from RP+ST^{LC} and RP+HPC liposomes was not significant ($P>0.05$). The release of FFAs confirmed the destruction of phospholipids that compose the liposome structure. The concentration of FFAs released increased rapidly in all formulations during the first 30 min of intestinal digestion, without reaching the maximum value in this time interval.

Our results indicate that LF facilitated the release of FFAs in RP+ST and RP+HPC+ST liposomes (Fig. 4b–d). Similar results were observed by Liu et al. (2017) who found that in liposomes composed of L–α–phosphatidylcholine and cholesterol LF facilitated the release of FFAs and increased the microfluidity of the bilayers, reducing the structural integrity. These findings concurred with the observation made by Sarkar, Horne, and Singh (2010) who showed that LF–stabilized in oil–in–water emulsions (soy oil) was more susceptible than other emulsions to lipolysis by pancreatic lipase. This effect can be attributed to polymers such as LF that could form a broad network allowing the localization of bile salts at the phospholipid bilayers interface increasing the fluidity of the membrane (Wilde & Chu, 2011). Bile salts at the interface would increase lipase adsorption damaging the structural organization of liposomes. It is noted that pancreatin is not only source of intestinal lipase but it also contains protease, trypsin, ribonuclease, and amylase activity. Therefore, while lipase would be responsible of phospholipids hydrolysis, proteases would

hydrolyze LF. At pH close to 7, protons are released during protein hydrolysis by proteases decreasing the pH. On the other hand, in RP+ST and RP+HPC+ST liposomes without LF (Fig. 4b–d), the FFAs release was slower and lower after 30 min of digestion. The increase of the concentrations of RP, HPC, and ST would increase the viscosity of the medium decreasing the movement of the lipase molecules towards the surface of the liposomes. An increase in the number of total liposomal particles could lead to a higher lipid surface available for the enzyme adsorption will decrease the rate of lipolysis in the bilayer, since the amount of enzyme is the same for the liposomal formulation with low (RP+ST^{LC}) and high (RP+ST, RP+HPC, and RP+HPC+ST) lipid concentration. For RP+ST^{LC} liposomes (Fig. 4a) the results obtained (0.05 ± 0.01 mM with LF and 0.04 ± 0.01 mM without LF) presented non–significant differences; this was explained by the low lipid concentration.

The high percentage of unsaturated fatty acids in RP could also be responsible for the fast hydrolysis rate of liposomes during the first 30 min of intestinal digestion. In general, the fatty acid composition and the type of phospholipids play an important role in lipid hydrolysis. For instance, phosphatidylserine and phosphatidylinositol are more susceptible to lipase hydrolysis than phosphatidylcholine and phosphatidylethanolamine (Liu, Ye, Han, & Han, 2019). This could explain the behavior exhibited by RP+HPC liposomes (Fig. 4c) in both the SDS–PAGE patterns and the amount of FFAs released. Membranes of RP+HPC liposomes would be more compacted given by the presence of 18: 0 DSPC and 16: 0 PSPC, in HPC, compared with those in RP+ST^{LC}, RP+ST, and RP+HPC+ST liposomes.

Finally, it is essential to consider that an optimum relation between liposome stability and destabilization is necessary for the LF release during digestion. Liposomal particles

511 elaborated with RP may be useful to modulate LF stability and offer a platform to deliver
512 intact LF in the intestine.
513
514 **4. Conclusions**
515 This work provides a characterization of lipid bilayer membrane in terms of structural
516 organization and contributes to increase the knowledge about the protection offered to LF
517 by different liposomal formulations against gastrointestinal digestion. Analysis of the lipid
518 organization in terms of chain conformational order, lateral packing, and lipid phase
519 transitions explains the stability performance of RP+ST^{LC} liposomes on LF encapsulation.
520 RP+ST, RP+HPC, and RP+HPC+ST liposomes can be used to encapsulate LF, to improve
521 its stability delaying its hydrolysis during gastric and intestinal digestion. The release of
522 FFAs during *in vitro* intestinal digestion, indicated that the phospholipids in the liposomes
523 were hydrolyzed and LF accelerated lipolysis from RP+ST and RP+HPC+ST liposomes.
524 On the whole, these results allowed envisaging these liposome formulations as a potential
525 system for the oral delivery of LF and possibly to other functional proteins. Future work
526 should be aimed to check antimicrobial bioactivity of digested LF–loaded into RP+ST,
527 RP+HPC, and RP+HPC+ST liposomes, and to evaluate the effect of these formulations on
528 the intestinal bacterial population, i.e. the prebiotic effect of the protein.
529
530 **Acknowledgements**
531 This research was supported by funds from CONICYT through CONICYT Doctoral
532 Scholarship 21161448; the Centre of Biotechnology and Bioengineering (CeBiB) FB–0001
533 and MINECO RTC–2016–4957–1 project. In addition, we would like to acknowledge the

Department of Chemical and Surfactant Technology at Institute of Advanced Chemistry of Catalonia (IQAC–CSIC), Barcelona, Spain; the Department of Chemical Engineering, and the Scientific and Technological Bioresource Nucleus (BIOREN) at Universidad de La Frontera, Temuco, to Jaume Caelles, Sonia Pérez, and Lidia Delgado for the expert technical assistance. Authors are also grateful to Lipoid GmbH for kindly providing Phospholipon® 90H.

Conflict of interest

The authors declare no conflict of interest.

Appendix A. Supplementary data

Supplementary data to this article can be found in Supplementary Data 1.docx

References

Andrade, M., Oseliero, P. L., Garcia, C., Sinigaglia-Coimbra, R., Pinto, C. L., & Pinho, S. C. (2018). Structural characterization of multilamellar liposomes coencapsulating curcumin and vitamin D3. *Colloids and Surfaces A*, *549*, 112–121.

Boland, M. (2016). Human digestion – a processing perspective. *Journal of the Science of Food and Agriculture*, *96*, 2275–2283.

Bragg, W. L. (1913). The diffraction of short electromagnetic waves by a crystal. *Proceedings of the Cambridge Philosophical Society*, *17*, 43–57.

De Figueiredo, G., Guedes, K., Paim, C., & Lopes, R. (2018). *In vitro* digestibility of heteroaggregated droplets coated with sodium caseinate and lactoferrin. *Journal of Food Engineering, 229,* 86–92.

Gibis, M., Ruedt, C., & Weiss, J. (2016). *In vitro* release of grape–seed polyphenols encapsulated from uncoated and chitosan–coated liposomes. *Food Research International, 88,* 105–113.

Gupta, S., De Mel, J. U., & Schneider, G. (2019). Dynamics of liposomes in the fluid phase. *Current Opinion in Colloid & Interface Science, 42,* 121–136.

Iglesias-Figueroa, B. F., Espinoza-Sánchez, E. A., Siqueiros-Cendón, T. S., & Rascón-Cruz, Q. (2019). Lactoferrin as a nutraceutical protein from milk, an overview. *International Dairy Journal 89,* 37–41.

Jafari, S. M., & McClements, D. J. (2017). Chapter One - Nanotechnology Approaches for Increasing Nutrient Bioavailability. *Advances in Food and Nutrition Research, 81,* 1–30.

Jovanović, A. A., Balanč, B. D., Ota, A., Grabnar, P. A., Djordjević, V. B., Šavikin, K. P., Bugarski, B. M., Nedović, V. A., & Ulrih N. P. (2018). Comparative effects of cholesterol and β-sitosterol on the liposome membrane characteristics. *European Journal of Lipid Science and Technology, 120*(9), 1800039.

Kaddaha, S., Khreich, N., Kaddah, F., Charcosset, C., & Greige-Gerges, H. (2018). Cholesterol modulates the liposome membrane fluidity and permeability for a hydrophilic molecule. *Food and Chemical Toxicology, 113,* 40–48

Kiselev, M. A., & Lombardo, D. (2017). Structural characterization in mixed lipid membrane systems by neutron and X-ray scattering. *Biochimica et Biophysica Acta, 1861*, 3700–3717.

Kokkona, M., Kallinteri, P., Fatouros, D., & Antimisiaris, S. G. (2000). Stability of SUV liposomes in the presence of cholate salts and pancreatic lipases: effect of lipid composition. *European Journal of Pharmaceutical Sciences, 9,* 245–252.

Laemmli, U. (1970). Cleavage of structural proteins during the assembly of the head of bacteriophage T4. *Nature, 227,* 680–685.

Liu, W., Ye, A., Han, F., & Han, J. (2019). Advances and challenges in liposome digestion: Surface interaction, biological fate, and GIT modeling. *Advances in Colloid and Interface Science, 263,* 52–67.

Liu, W., Ye, A., Liu, W., Liu, C., & Singh, H. (2013). Stability during *in vitro* digestion of lactoferrin–loaded liposomes prepared from milk fat globule membrane–derived phospholipids. *Journal of Dairy Science, 96,* 2061–2070.

Liu. W., Wei, F., Ye, A., Tian, M., & Han, J. (2017). Kinetic stability and membrane structure of liposomes during *in vitro* infant intestinal digestion: Effect of cholesterol and lactoferrin. *Food Chemistry, 230,* 6–13.

López, O., de la Maza, A., Coderch, L., López-Iglesias, C., Wehrli, E., & Parra, J. L. (1998). Direct formation of mixed micelles in the solubilization of phospholipidliposomes by Triton X-100. *FEBS Letters, 426,* 314–318.

Machado, A. R., Pinheiro, A. C., Vicente, A. A., Souza–Soares, L. A., & Cerqueira, M. A. (2019). Liposomes loaded with phenolic extracts of Spirulina LEB–18: Physicochemical

598 characterization and behavior under simulated gastrointestinal conditions. *Food Research*
599 *International*, *120*, 656–667.
600 **Maherani, B., Arab–Tehrany, E., Kheirolomoom, A., Geny, D., & Linder, M.** (2013).
601 Calcein release behavior from liposomal bilayer; influence of
602 physicochemical/mechanical/structural properties of lipids. *Biochimie, 95*(11), 2018–2033.
603 **McClements, D. J.** (2016). Interfacial properties and their characterization. Food
604 emulsions: Principles, practices, and techniques. (3rd ed.). Taylor & Francis Group. Boca
605 Raton, FL: CRC Press. pp. 185–244.
606 **Meshulam, D., & Lesmes, U.** (2014). Responsiveness of emulsions stabilized by
607 lactoferrin nano-particles to simulated intestinal conditions. *Food & Function, 5*, 65–73.
608 **Neunert, G., Tomaszewska–Gras, J., Siejak, P., Pietralik, Z., Kozak, M., & Polewski,**
609 **K.** (2018). Disruptive effect of tocopherol oxalate on DPPC liposome structure: DSC,
610 SAXS, and fluorescence anisotropy studies. *Chemistry and Physics of Lipid, 216*, 104–113.
611 **Niu, Z., Loveday, S. M., Barbe, V., Thielen, I., He, Y., & Singh, H.** (2019). Protection of
612 native lactoferrin under gastric conditions through complexation with pectin and chitosan.
613 *Food hydrocolloids, 93*, 120–130.
614 **Rahnfeld, L., Thamm, J., Steiniger, F., van Hoogevest, P., & Luciani, P.** (2018). Study
615 on the in situ aggregation of liposomes with negatively charged phospholipids for use as
616 injectable depot formulation. *Colloids and Surfaces B: Biointerfaces*, *168*, 10–17.
617 **Rodríguez, G., Cócera, M., Rubio, L., Alonso, C., Pons, R., Sandt, C., Dumas, P.,**
618 **López–Iglesias, C., de la Maza, A., & López, O.** (2012). Bicellar systems to modify the
619 phase behaviour of skin stratum corneum lipids. *Physical Chemistry Chemical Physics, 14*,
620 14523–14533.

Romero-Arrieta, M. R., Uria-Canseco, E., & Perez-Casas, S. (2019). Simultaneous encapsulation of hydrophilic and lipophilic molecules in liposomes of DSPC. *Thermochimica Acta, In Press, Corrected Proof,* 178462.

Sarkar, A., Horne, D. S., & Singh, H. (2010). Pancreatin–induced coalescence of oil–in–water emulsions in an *in vitro* duodenal model. *International Dairy Journal, 20*, 589–597.

Sun, N., Chen, J., Wang, D., Lin, S. (2018). Advance in food-derived phospholipids: Sources, molecular species and structure as well as their biological activities. *Trends in Food Science & Technology, 80*, 199–211.

Troost, F. J., Saris, W. H. M., & Brummer, R. J. M. (2002). Orally ingested human lactoferrin is digested and secreted in the upper gastrointestinal tract *in vivo* in women with ileostomies. *Journal of Nutrition, 132*, 2597–2600.

Vélez, M. A., Perotti, M. C., Zanel, P., Hynes, E. R., & Gennaro, A. M. (2017). Soy PC liposomes as CLA carriers for food applications: Preparation and physicochemical characterization. *Journal of Food Engineering, 212*, 174–180.

Vergara, D., & Shene, C. (2019). Encapsulation of lactoferrin into rapeseed phospholipids based liposomes: optimization and physicochemical characterization. *Journal of Food Engineering, 262*, 29–38.

Wilde, P. J., & Chu, B. S. (2011). Interfacial & colloidal aspects of lipid digestion. *Advances in Colloid and Interface Science, 165,* 14–22.

Yao, X., Bunt, C., Cornish, J., Quek, S. Y., & Wen, J. (2015). Oral delivery of bovine lactoferrin using pectin– and chitosan–modified liposomes and solid lipid particles: improvement of stability of lactoferrin. *Chemical Biology & Drug Design*, *86*(4), 466–477.

Zhang, J., Han, J., Ye, A., Liu, W., Tian, M., Lu, Y., Wu, K., Liu, J., & Lou M. P. (2019b). Influence of phospholipids structure on the physicochemical properties and *in vitro* digestibility of lactoferrin-loaded liposomes, *Food Biophysics, 14*, 287–299.

Zhang, Y., Pu, C., Tang, W., Wang, S., & Sun, Q. (2019a). Gallic acid liposomes decorated with lactoferrin: Characterization, *in vitro* digestion and antibacterial activity. *Food Chemistry*, *293*(30), 315–322.

Credit author statement

Daniela Vergara, funding acquisition, conceptualization, methodology, formal analysis, writing - original draft. **Olga López,** supervision, resources, writing - review and editing. **Mariela Bustamante,** resources. **Carolina Shene,** funding acquisition, supervision, writing - review and editing.

Table 1. Composition of RP liposomes submitted to *in vitro* gastrointestinal digestion.

	mg/mL		
Formulation	**RP**	**ST**	**HPC**
RP+ST^{LC}	10.20	2.20	--
RP+ST	25.50	5.50	--
RP+HPC	25.50	--	5.50
RP+ST+HPC	21.70	3.10	6.20

RP, rapeseed phospholipids; ST, stigmasterol; ^{LC,} low concentration; and HPC, hydrogenated phosphatidylcholine.

Table 2. Residual LF after the incubation of RP+ST^{LC}, RP+ST, RP+HPC, and RP+HPC+ST–liposomes, with the gastric and intestinal fluid (GF and IF) and after gastric and intestinal digestion (GD and ID), based on relative measurements from the SDS–PAGE. Values are means ± standard deviations (n≥3). The numbers 1', 30', and 120' represent the sampling time (min). Different superscript letters indicate significant differences (P<0.05) for LF in the different liposomes in the column (n=3).

	LF (%)			
Sample	**GF**	**GD**		
	120'	**1'**	**30'**	**120'**
Free LF	92.16 ± 1.80^{a}	89.43 ± 3.30^{a}	34.98 ± 3.85^{c}	0.00 ± 0.00^{d}
LF–loaded RP+ST^{LC}	81.08 ± 1.22^{ab}	89.22 ± 3.18^{a}	46.43 ± 0.08^{c}	20.48 ± 3.57^{c}
LF–loaded RP+ST	74.71 ± 0.72^{a}	69.51 ± 3.07^{a}	67.92 ± 1.90^{b}	67.49 ± 1.79^{b}
LF–loaded RP+HPC	74.94 ± 6.66^{a}	88.83 ± 9.03^{a}	85.42 ± 5.76^{a}	79.98 ± 1.82^{a}
LF–loaded RP+ST+HPC	83.05 ± 6.55^{a}	69.93 ± 0.71^{a}	69.66 ± 0.99^{b}	67.51 ± 0.24^{b}
Sample	**IF**	**ID**		
	120'	**1'**	**30'**	**120'**
Free LF	81.38 ± 0.08^{a}	14.89 ± 0.88^{b}	12.65 ± 0.19^{c}	10.18 ± 1.10^{c}
LF–loaded RP+ST^{LC}	83.25 ± 1.69^{a}	21.95 ± 0.47^{a}	13.29 ± 0.64^{c}	10.88 ± 0.60^{bc}
LF–loaded RP+ST	89.66 ± 4.18^{a}	16.16 ± 1.66^{b}	20.34 ± 0.32^{a}	34.80 ± 0.65^{a}
LF–loaded RP+HPC	94.44 ± 1.19^{a}	19.07 ± 1.96^{ab}	17.36 ± 1.36^{b}	32.19 ± 1.87^{a}
LF–loaded RP+HPC+ST	81.53 ± 7.13^{a}	16.52 ± 0.76^{b}	16.17 ± 0.02^{b}	15.85 ± 1.56^{b}

RP, rapeseed phospholipids; ST, stigmasterol; ^{LC}, low concentration; HPC, hydrogenated phosphatidylcholine; GF, gastric fluid (without pepsin); GD, gastric digestion (with pepsin); IF, intestinal fluid (without pancreatin); ID, intestinal digestion (with pancreatin).

Figure captions

Fig. 1. Characterization of RP+ST^{LC} liposomes. X-ray scattering profile of. (a) Small angle X-ray scattering (SAXS); (b) Wide angle X-ray scattering (WAXS); (c-d) Differential scanning calorimetry (DSC) thermograms; (e-f) Cryo–TEM micrographs.

Fig. 2. Physicochemical stability of RP+ST^{LC} liposomes in gastric (□) and intestinal (○) fluid; gastric (pepsin) digestion (■) and intestinal (pancreatin) digestion (●), (a-b) particle size, (c-d) polydispersity index (PDI), and (e-f) ζ–potential.

Fig. 3. SDS–PAGE patterns of free LF and LF–loaded into RP+ST^{LC}, RP+ST, RP+HPC, and RP+HPC+ST liposomes under (a) gastric and (b) intestinal conditions. Lanes: MW, molecular weight standard; LF, free lactoferrin (standard); GF, gastric fluid (without pepsin); GD, gastric digestion (with pepsin); IF, intestinal fluid (without pancreatin); ID, intestinal digestion (with pancreatin). The numbers 1, 30, and 120 represent the sampling time (min).

Fig. 4. Concentration profile of the free fatty acids (FFAs) released during *in vitro* intestinal digestion of (a) RP+ST^{LC}, (b) RP+ST, (c) RP+HPC, and (d) RP+HPC+ST liposomes with (●) or without (○) LF.

Fig. 1

Click here to download high resolution image

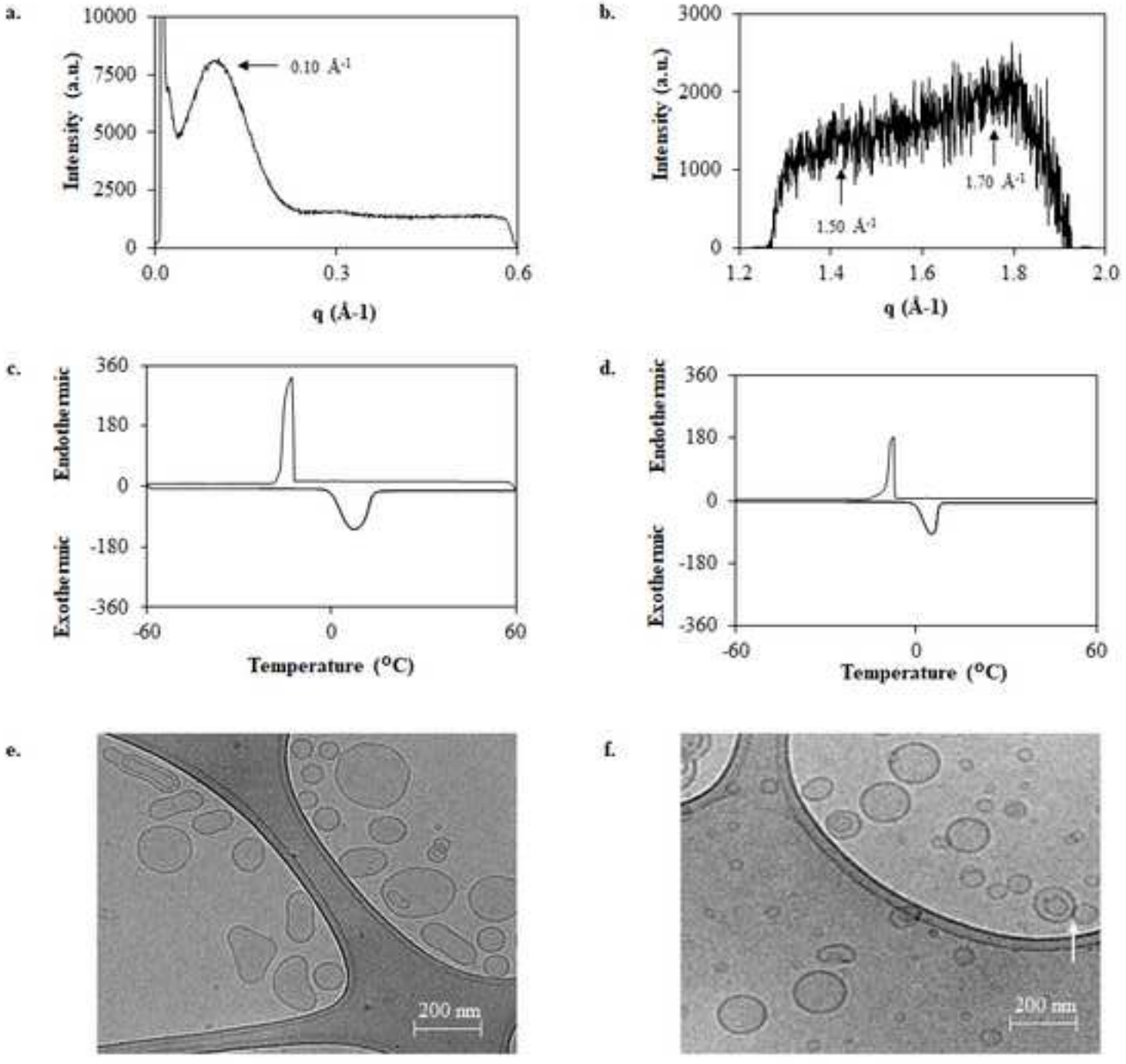

Fig. 2

Click here to download high resolution image

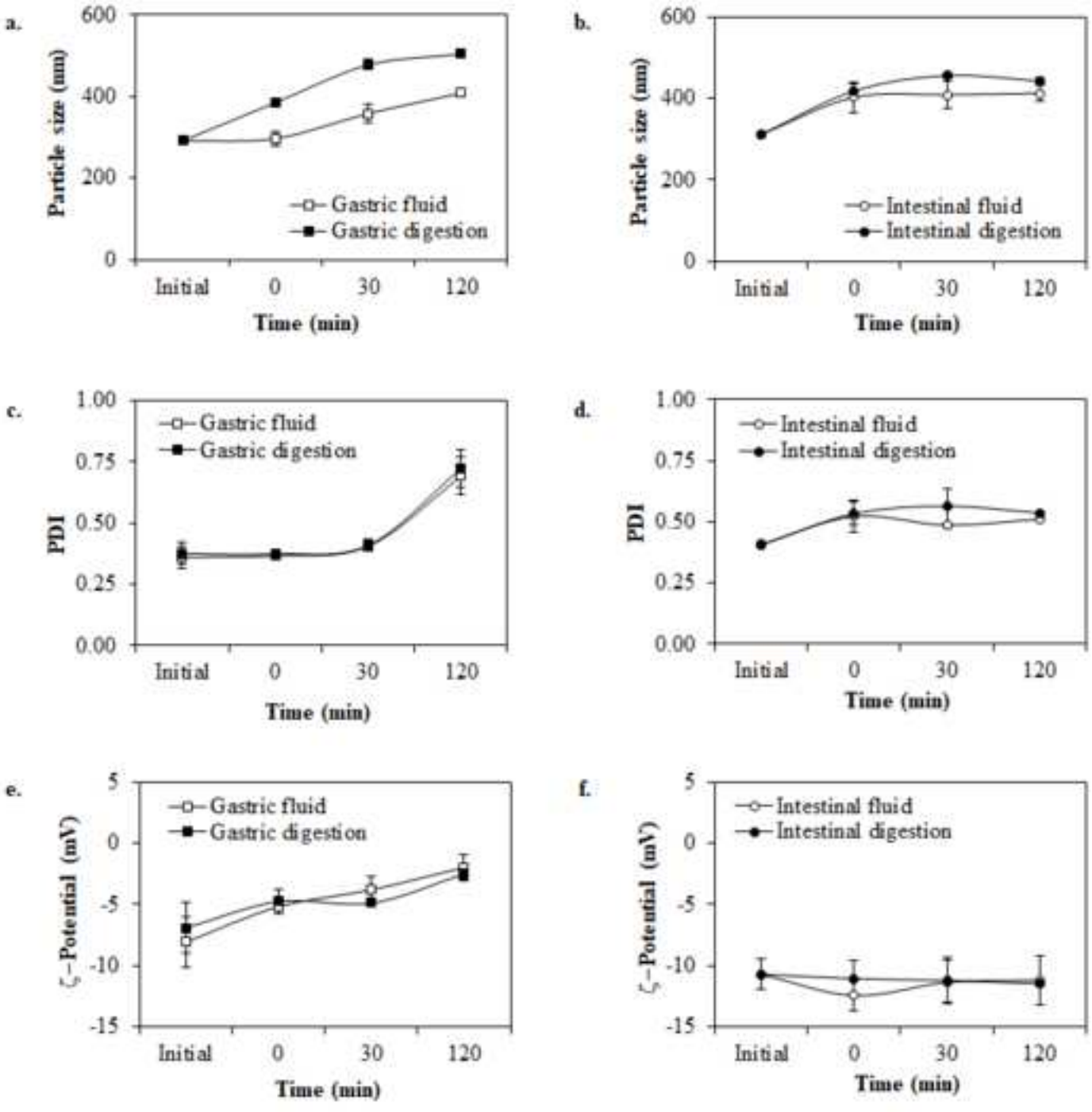

Fig. 3

Click here to download high resolution image

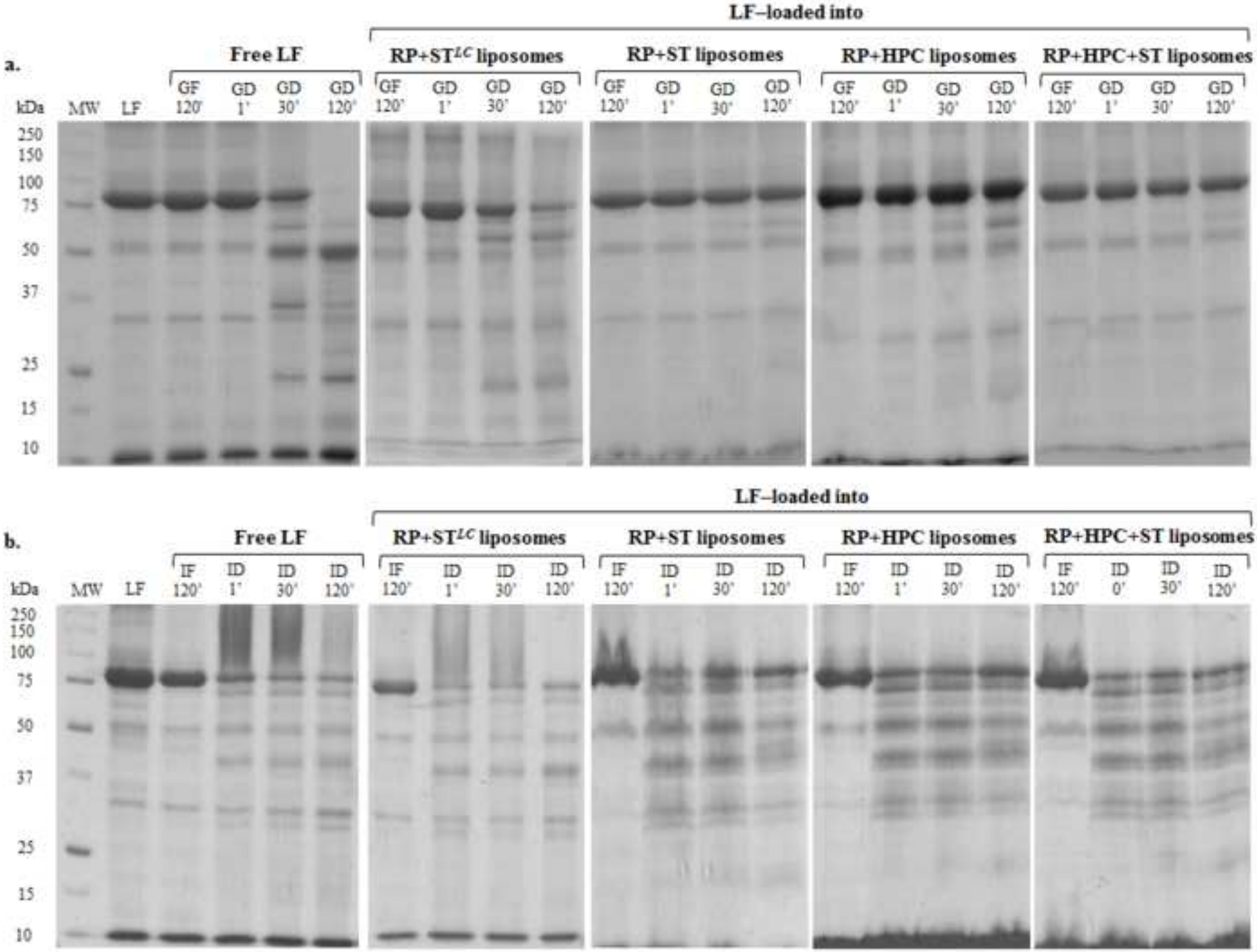

Fig. 4

Click here to download high resolution image

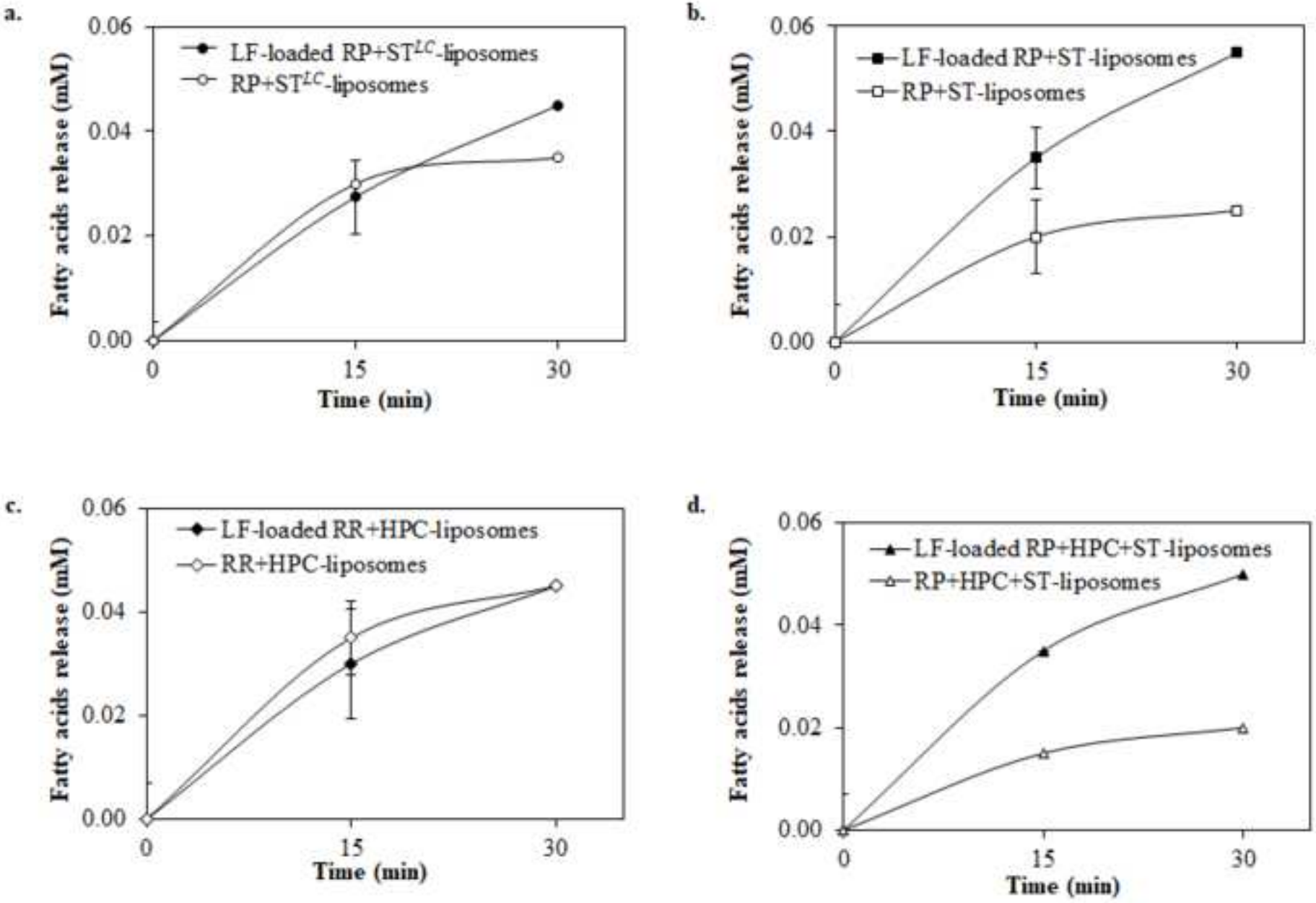

An *in vitro* digestion study of encapsulated lactoferrin in rapeseed phospholipid–based liposomes

Daniela Vergara[a,b*], Olga López[d], Mariela Bustamante[b], Carolina Shene[b,c]

[a] *Doctoral Program in Sciences of Natural Resources, Universidad de La Frontera, Ave. Francisco Salazar 01145, Box 54-D, Temuco, Chile.*

[b] *Center of Food Biotechnology and Bioseparations, Scientific and Technological Bioresource Nucleus (BIOREN), Centre for Biotechnology and Bioengineering (CeBiB). Universidad de La Frontera, Ave. Francisco Salazar 01145, Box 54-D, Temuco, Chile.*

[c] *Department of Chemical Engineering, Universidad de La Frontera, Ave. Francisco Salazar 01145, Box 54-D, Temuco, Chile.*

[d] *Department of Chemical and Surfactant Technology, Institute of Advanced Chemistry of Catalonia (IQAC-CSIC), C/Jordi Girona 18-26, 08034, Barcelona, Spain.*

*Corresponding author: Tel.: +56 45 2325491; fax: +56 45 2732402

E-mail address: d.vergara02@ufromail.cl (D. Vergara).

Table S1. Composition of rapeseed oil used for phospholipids extraction.

Composition	**Rapeseed oil**
Humidity (%)	0.5 max.
Impurity (%)	0.5 max.
Peroxide index (meq O_2)	2 max.
Oleic acid (C18:1) (%)	50–70
Linoleic acid (C18:2) (%)	20–22
Linolenic acid (C18:3) (%)	8–12
Trans fatty acids	0.1 max.
Erucic acid (%)	< 0.5
Glucosinolates (µmol/g)	< 9

Table S2. Composition of rapeseed phospholipids (RP) used in liposome production.

	RP
Phosphorus content (g/kg)	1.88 ± 0.09
Proximate analysis (%)	
Moisture	1.07 ± 0.03
Volatile components	88.66 ± 0.13
Fixed carbon	1.41 ± 0.10
Ash	8.74 ± 0.28
Phospholipids mg/g	
Phosphatidylcholine (PC)	26.42 ± 0.24
Phosphatidylethanolamine (PE)	122.98 ± 3.78
Phosphatidic acid (PA) + Lysophosphatidylcholine (LPC)	126.94 ± 18.71
Fatty acid (%)	
Palmitic acid (C16:0)	7.84 ± 0.02
Stearic acid (C18:0)	1.27 ± 0.03
Oleic acid (C18:1)	55.02 ± 0.06
Linoleic acid (C18:2)	27.97 ± 0.07
α-Linolenic acid (C18:3)	6.26 ± 0.01
Others	1.64 ± 0.00
Tocopherols (mg/100 g)	
α-tocopherol	17.05 ± 2.93
δ-tocopherol	50.03 ± 3.32
γ-tocopherol	10.59 ± 0.71
Amino acids (mg/100 g)	
Arginine	14.97 ± 2.56
Histidine	79.53 ± 3.56
Proline	119.93 ± 9.87

Taken/adapted from Vergara and Shene, (2019)

***Declaration of Interest Statement**

Declaration of interests

☒ The authors declare that they have no known competing financial interests or personal relationships that could have appeared to influence the work reported in this paper.

☐The authors declare the following financial interests/personal relationships which may be considered as potential competing interests: